Mat. Res. Soc. Symp. Proc. Vol. 635 © 2001 Materials Research Society

Optical Response of Gold Nanoparticles in Dielectric Materials

Akira Ueda, Elana M. Bryant, Carlton B. Maxwell, Charline M. Blake, Richard R. Mu, Marvin H. Wu, Andrey I. Zavalin, Alkiviathes Meldrum[1] and Don O. Henderson
Chemical Physics Laboratory, Department of Physics, Fisk University, Nashville, TN 37208, USA
[1]Department of Physics, University of Alberta, Edmonton, Alberta, Canada

ABSTRACT

The fundamental studies of metallic nanoparticles embedded in various host materials have been made. The host-guest interaction causes the shapes of embedded nanoparticles, and the surface plasmon resonances of the metallic nanoparticles are affected by the host materials. The control of the surface plasmon resonance condition is a challenging question. We will discuss the interface effect of the systems where gold nanoparticles were fabricated between materials of MgO and SiO_2.

INTRODUCTION

Surface plasmon resonance (SPR) of small metallic particles has been studied since Mie's calculation of 1908 about the study [1] of optical properties of gold particles, and in the past three decades the new field of cluster science has been developed with many potential applications. Although many studies have been published, there are still new interesting systems and there are fundamental questions to be answered. In our laboratory, we have studied the systems of several insulating materials implanted with gold ions (Al_2O_3:Au, CaF_2:Au, Silica SiO_2:Au, MgO:Au, Muscovite Mica:Au, and Vycor Glass:Au) and of the porous materials impregnated with gold (Vycor Glass: Au)[2-5].

In the systems of SiO_2:Au and MgO:Au fabricated by ion implantation, we have previously seen the growth of gold nanocrystals and found the SPR positions to be 530 nm and 560 nm, respectively, after a suitable thermal annealing in 5%O_2+95%Ar atmosphere. These SPR positions agree with the Mie's theory using a dipole approximation (Flölich approximation) for spherical particles, that satisfies the following equation:

$$\varepsilon(\omega_{SP}) + 2\varepsilon_m = 0, \qquad (1)$$

where $\varepsilon(\omega)$ is the dielectric function of gold, ε_m is the dielectric function of host material, and ω_{SP} is the surface plasmon frequency.

As shown in Fig. 1, from our previous experiments, the gold nanocrystals in MgO have rounded cubic shape with a side-length of 10 nm or less, that aligns along the crystal axis of MgO (100), while the gold nanocrystals in silica glass (SiO_2) are spherical. (The detail of this result will be discussed elsewhere.) If only the surface energy of gold particles plays the dominant role for the nanocrystal growth, the shape should be spherical. The host MgO crystal, therefore, must contribute to this result of cubic gold particles because MgO single crystal has a cubic crystal structure. Fuchs has investigated the optical absorption of small ionic crystalline cubes in infrared region by calculating the normal modes of the surface polarization charges [6]. For cubes, he found that several surface polariton mode conditions for the dielectric function ranges $-3.68\varepsilon_m \leq \varepsilon(\omega_{SP}) \leq -0.42\varepsilon_m$, instead of the sphere condition of Eq.(1): $\varepsilon(\omega_{SP}) = -2\varepsilon_m$. The strongest mode satisfies the condition: $\varepsilon(\omega_{SP}) = -3.68\varepsilon_m$. It is expected that metallic cubes follow the similar conditions, and this corresponding strongest mode for a gold cube embedded in MgO is approximately located

at 680 nm. The shape of observed gold particles is rounded cube, so that the resonance condition for SPR might be $-3.68\varepsilon_m \leq \varepsilon(\omega_{SP}) \leq -2\varepsilon_m$.

On the other hand, if the distance between gold particles is short enough, gold particles are no longer regarded as isolated particles and the induced dipole-dipole interaction may result in an absorption band at longer wavelength.

In this paper, we will discuss the interfacial interaction between gold nanocrystals and the dielectric hosts mainly by observing the SPR band of the systems.

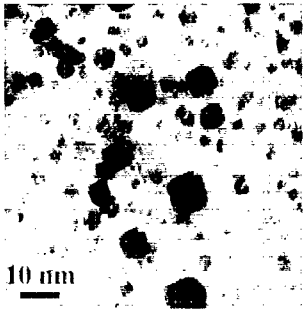

Figure 1 TEM image of Gold nanocrystals fabricated in MgO single crystal by ion implantation with a post annealing. The shape of the gold nanocrystals is rounded cubic and they align along the crystal axis of host MgO (100).

EXPERIMENTAL

MgO substrates were single crystal plates (1" x 1" x 0.5 mm) with polished (100) surface obtained from Princeton Scientific Corporation. Gold was deposited onto the substrates by electron beam evaporation in a vacuum with the pressure of ~ 10^{-7} torr. Overcoating with MgO and SiO_2 was carried out also by electron beam evaporation with thickness of 100 nm and a deposition rate of 0.5 Å/sec for both Au and MgO. UV-VIS spectra of the samples were taken before and after every thermal annealing with a spectrophotometer (Hitachi, U-3501). Thermal annealing was carried out with a tube furnace with Ar gas (99.995%) flow.

In order to see the matrix dependence, we fabricated the following three systems: (1)Au deposition of 50 Å on MgO substrate with a MgO overcoat [MA50M] , (2) Au deposition of 25 Å on MgO substrate with a MgO overcoat [MA25M]], and (3) Au deposition of 50 Å on MgO substrate with a SiO_2 overcoat [MA50S]. Hereafter, the abbreviations for the systems MA50M, MA25M, and MA50S will be used for simplicity: the each letter in the abbreviations from left to right represents the substrate material, gold deposition with the thickness in Å, and the overcoat materials, respectively. For reference purpose, we have made samples without overcoating and an Atomic Force Microscope (AFM) was used to image gold nanoparticles as well as surface of coating.

RESULTS AND DISCUSSIONS

Fig. 2 shows the annealing temperature dependence of the UV-VIS transmission spectra for two systems (a)MA50S and (b)MA50M. Each spectrum was taken from the same samples for (a)MA50S and (b)MA50M annealed sequentially as indicated. For both cases, at low annealing temperatures, there are SPR absorption bands tailing into longer wavelength, probably because the prepared sample consists of an island-type gold film with effective thickness of 50 Å. The gold film may not be ruptured to form gold particles at low temperatures. At 800°C, the absorption tail at longer wavelength suddenly became weaker and the SPR became sharper as the annealing temperature increased. This indicates that the gold film had been ruptured and formed nano-meter size gold particles in the system. For the system with MgO overcoat (MA50M), the SPR band dramatically decreased at 1100°C, which indicated that gold atoms escaped from the system through the thin overcoat with thickness of 100 nm.

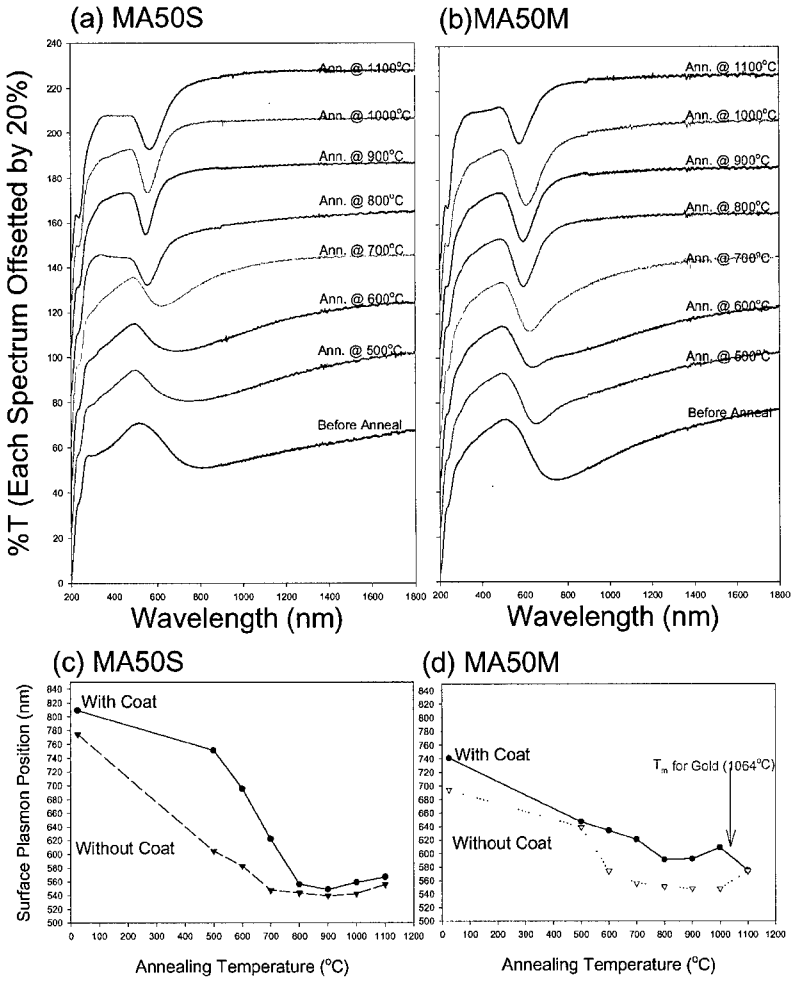

Figure 2 Annealing Temperature Dependence of UV-VIS Transmission Spectra for (a)MA50S and (b)MA50M and Surface Plasmon Position as a Function of Annealing Temperature for (c) MA50S and without Coating and (d) MA50M and without Coating.

The evolution of SPR position as a function of annealing temperature is plotted for each system of MA50S and MA50M accompanying un-coated samples as a reference, as shown in Fig. 2(c) and (d), respectively. For MA50S, the SPR positions became shorter as annealing temperature increased up to 800°C for both coated and un-coated system, and then it became nearly stable at 560 nm and 550 nm, for the coated and un-coated samples, respectively. Above 1000°C, the SPR positions slightly increased with the annealing temperature. For MA50M, the SPR positions gradually decreased as annealing temperature increased up to 800°C and then became stable. The SPR positions are 590 nm and 550 nm for coated and un-coated samples, respectively. At 1000°C, the coated sample increased SPR position slightly, and at 1100°C the positions merged together to 580 nm. Since the melting point of gold is 1064°C, gold could escape from the systems.

Similarly, Fig. 3(a) shows the annealing temperature dependence of the UV-VIS transmission spectra for system MA25M. Each spectrum was taken from the same sample of MA25M annealed sequentially as indicated. The evolution of SPR position as a function of annealing temperature is plotted for the system of MA25M accompanying un-coated sample as a reference, as shown in Fig. 3 (b). In this case, there is a weaker absorption tail at longer wavelength in comparison with systems MA50S and MA50M shown in Fig. 2. Since the starting effective thickness was 25 Å, the actual gold film was not uniform and probably a patched film that may contain nearly isolated gold particles. Thus the SPR position started from 645 nm and 625 nm for the coated and un-coated samples, respectively. However, the trend of evolution of spectra and SPR position are similar to those of system MA50M. The SPR positions in the stable region between 700°C and 900°C are 600 nm and 550 nm for the coated and un-coated samples, respectively. At 1000°C SPR position for the coated sample increased, and at 1100°C SPR positions for coated and un-coated samples merged together, as system MA50M behaved.

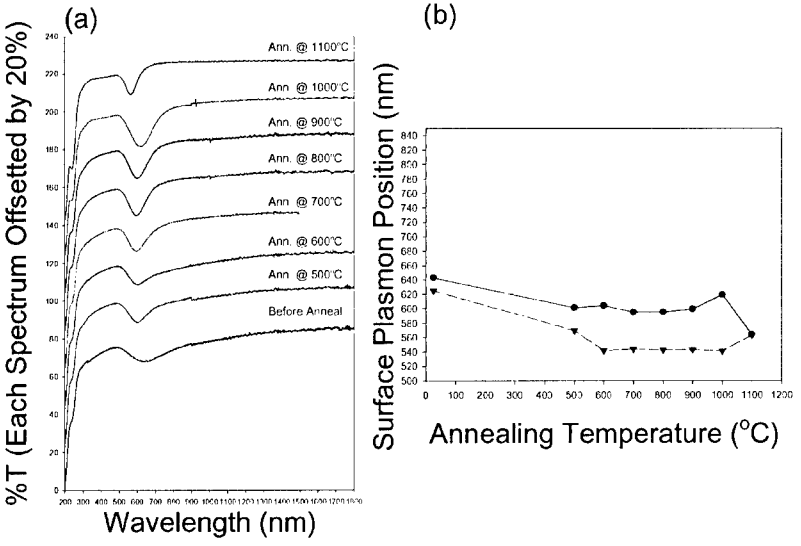

Figure 3 (a)Annealing Temperature Dependence of UV_VIS Transmission Spectra of the System MA25M and (b) SPR Position as a Function of Annealing Temperature.

Table 1 Summary of SPR Positions for Several Systems Obtained by Both Theoretical Calculation and Experiments.

	System	Particle Shape	SPR (nm)
Theoretical results	Au in MgO: $\varepsilon(\omega_S P)+2\varepsilon_{MgO}=0$	Sphere	550
	Au in SiO_2: $\varepsilon(\omega_S P)+2\varepsilon_{SiO2}=0$	Sphere	535
	Au in Vacuum: $\varepsilon(\omega_S P)+2\varepsilon_{Vac}=0$	Sphere	500
	Au in MgO: $\varepsilon(\omega_S P)+3.68\varepsilon_{MgO}=0$	Cube	680
Experimental results (After annealed up to 1000°C)	Au implanted in MgO	Cube	560 ±3
	Au implanted in SiO_2	Sphere	532 ±3
	MA50S	N/A	560 ±5
	MA50 (fabricated with MA50S)	Oblate Spheroid	550 ±5
	MA50M	N/A	590 ±5
	MA50 (fabricated with MA50M)	Oblate Spheroid	550 ±5
	MA25M	N/A	600 ±5
	MA25 (fabricated with MA25M)	Oblate Spheroid	550 ±5

In Table 1, a summary of SPR positions for several systems obtained by both theoretical calculation and experiments. SPR for spherical Au particle in vacuum is the minimum value in the table because of its dielectric constant (the electric permittivity for vacuum). The uncoated samples, MA50 and MA25, were exposed to the air whose dielectric constant is close to vacuum and have SPR position at a relatively longer wavelength. This suggested that the shape of Au particles is not sphere. The systems, MA50M and MA25M, have SPR at longer wavelengths than that of the Au implanted in MgO. Since there is a possibility to have anisotropic shape of gold particles at the interface in the systems, especially MAu50M and MAu25M, those particles have more likely oblate spheroid type shape. As a reference, we have imaged gold particles of un-coated samples with an AFM. Fig. 4 shows the development of gold particles on the sample of M50: (a) as-deposited, (b) after annealed at 1000°C, and (c) after annealed at 1100°C. According to the AFM cross-section analysis, the gold particles are semispherical or oblate spheroid shaped. The aspect ratios (height to diameter) of gold particles are 0.05-0.11 for (a), 0.20-0.23 for (b), and 0.22-0.33 for (c). A model calculation for oblate spheroid with an aspect ratio of 0.01-0.3 in the air gave the SPR position around 500 nm (Oblate spheroids have an upper limit of SPR in a certain medium, as a longest SPR wavelength.), while the experimental results for un-coated samples (MA50 and MA25) are about 550 nm. Since the systems of un-coated samples are gold particles on MgO, the substrate effect should be considered.

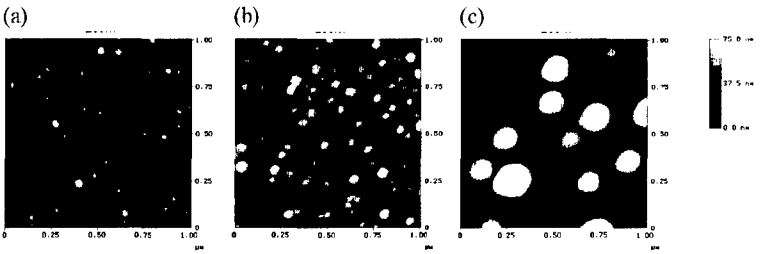

Figure 4 AFM Images of Gold Particles on an Un-coated Sample annealed at Different Temperatures: (a) as-deposited, (b) 1000°C, and (c) 1100°C. (The scan scales are all 1 μm x 1 μm.)

CONCLUSION

We have proposed the fabrication method of anisotropic gold particles. In order to manipulate the SPR position, we need to know the shape of gold particles in coated samples. At this stage, we did not obtain TEM images of the coated samples, and we need to know the crystal structure of coated MgO, as well. Furthermore, we need to take into account the interaction between gold particles.

REFERENCE

[1]G. Mie, Ann, Physik **25**, 377(1908). (German)

[2]D.O. Henderson, Y.-S. Tung, A. Ueda, R. Mu, Y. Xue, C. Hall, W.E. Collins, C.W. White, R.A. Zuhr, Jane G. Zhu, and P.W. Wang, J. of Vacuum Science and Technology **A 14**(3), 1199(1996); D.O. Henderson, Y.-S. Tung, R. Mu, A. Ueda, J. Chen, R. Gu, C.W. White, Jane G. Zhu, M. McKay, and O. Scott., International Conference of Defects in Insulating Materials, Wake Forest University, Winston-Salem, NC, USA, 1996. Materials Science Forum **239-241**, 695(1997).

[3]Z. Gu, R. Mu, A. Ueda, Y.-S. Tung, M.H. Wu, D.O. Henderson, A. Meldrum, C.W. White, and R.A. Zuhr, JVST **A16**,1409(1998).

[4]A. Ueda, D.O. Henderson, R. Mu, Y.-S. Tung, C.W. White, Jane G. Zhu, International Conference of Defects in Insulating Materials, Wake Forest University, Winston-Salem, NC, USA, 1996. Materials Science Forum **239-241**, 675(1997).

[5]D.O. Henderson, R. Mu, A. Ueda, Y.-S. Tung, C.W. White, R.A. Zuhr, and Jane G. Zhu, J. of Non-Crystalline Solids, **205/207**, 788(1996). The Ninth International Conference on Liquid and Amorphous Metal, Chicago, IL October 8-13, 1995, Proceedings; Y.-S. Tung, R. Mu, D.O. Henderson, A. Ueda, C.W. White, Jane G. Zhu, International Conference of Defects in Insulating Materials, Wake Forest University, Winston-Salem, NC, USA, 1996. Materials Science Forum **239-241**, 691(1997).

[6]Fuchs, Phys. Rev. **B11**, 1732 (1975); U. Kreibig and M. Vollmer, "Optical Properties of Metal Clusters," Springer Series in Materials Science 25 (Springer, New York, 1995).